Supplementary Materials for: Spatially resolved neural slowing predicts impairment and amyloid burden in Alzheimer's disease

Alex I. Wiesman[1,2*], Daniel L. Murman[2,3], Rebecca A. Losh[4], Mikki Schantell[4], Nicholas J. Christopher-Hayes[4], Hallie J. Johnson[4], Madelyn P. Willett[4], Sara L. Wolfson[5], Kathryn L. Losh[4], Craig M. Johnson[6], Pamela E. May[2], Tony W. Wilson[4]

Author affiliations:

[1] Montreal Neurological Institute, McGill University, Montreal, QC, CA
[2] Department of Neurological Sciences, University of Nebraska Medical Center (UNMC), Omaha, NE, USA
[3] Memory Disorders & Behavioral Neurology Program, UNMC, Omaha, NE, USA
[4] Institute for Human Neuroscience, Boys Town National Research Hospital, Boys Town, NE, USA
[5] Geriatrics Medicine Clinic, UNMC, Omaha, NE, USA
[6] Department of Radiology, UNMC, Omaha, NE, USA
[*] Corresponding Author

Correspondence to:

Alex I. Wiesman, Ph.D.
Montreal Neurological Institute
McGill University
845 Sherbrooke St W
Montreal, Quebec H3A 0G4
alexander.wiesman@mcgill.ca

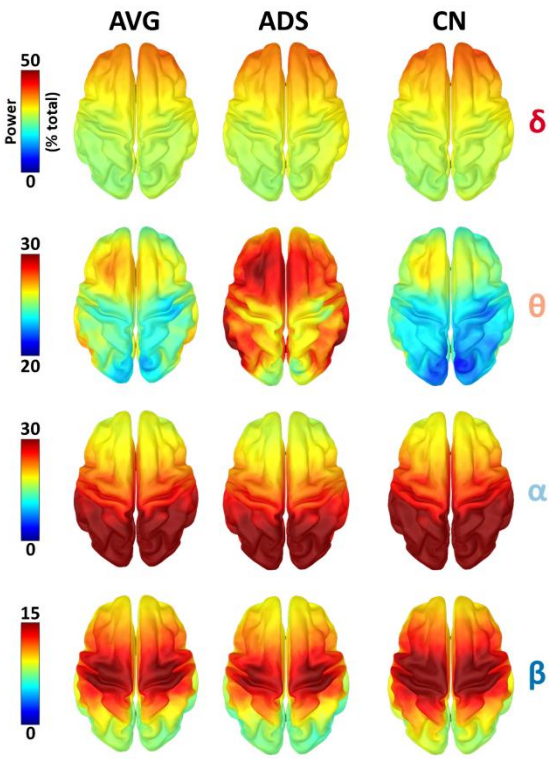

Figure S1. Averaged cortical spectral amplitude maps per group. Surface maps represent source-imaged spectral amplitude data averaged over all participants (left), as well as within each participant group (Alzheimer's disease spectrum (ADS): middle; cognitively normal (CN): right). Scale bars to the far left indicate relative amplitude (in % total spectral power) for each frequency band denoted on the far right.

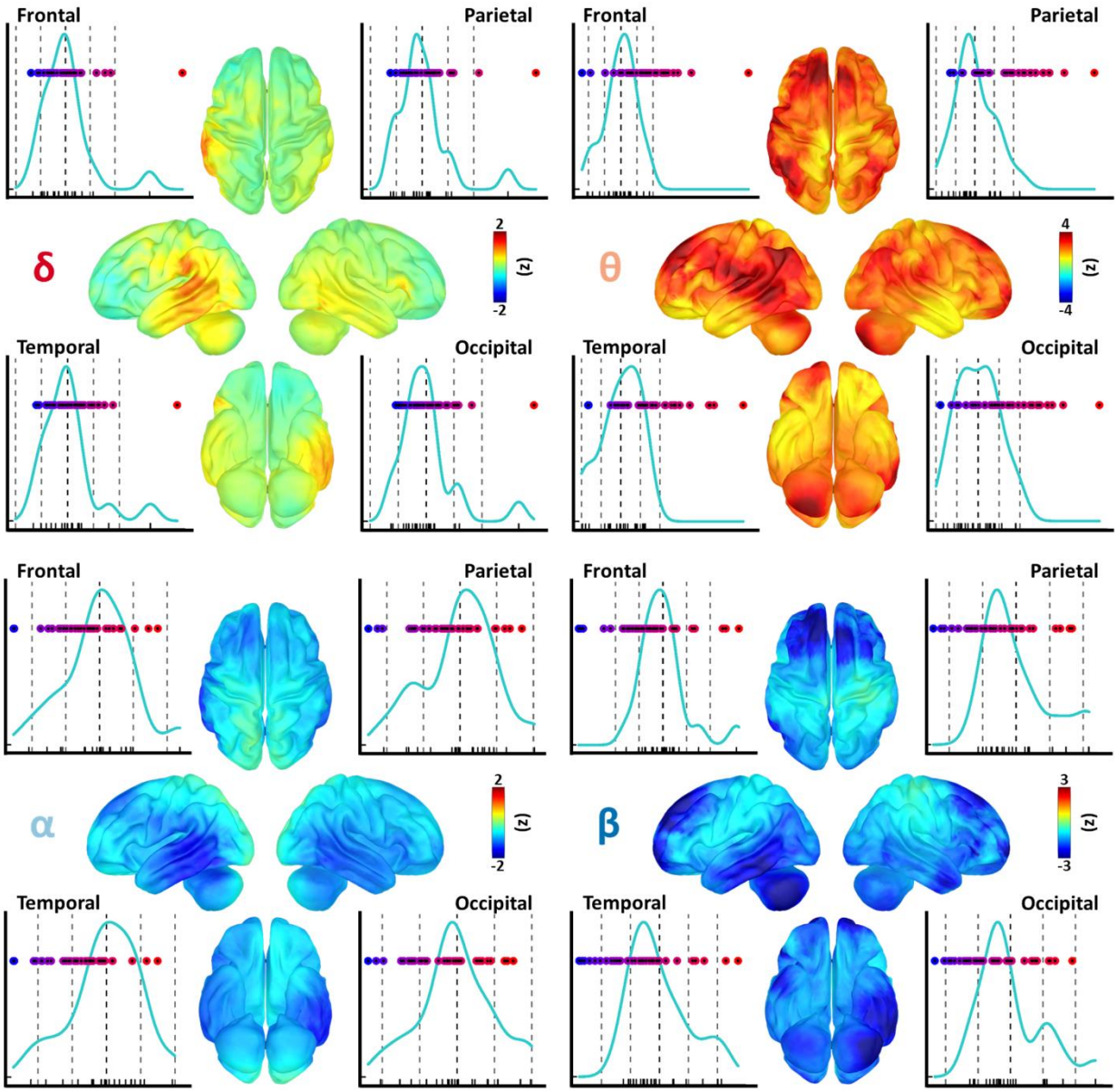

Figure S2. Patient spectral deviations per frequency band and lobe. To standardize the source-imaged spectral amplitude maps per frequency, vertex-wise data for each patient were normalized to the distribution of the comparable data (i.e., the same frequency and vertex) from the cognitively normal group. The resulting patient spectral deviation maps are displayed, per frequency band, as grand-averages across the Alzheimer's disease spectrum group on the cortical surfaces shown above. The frequency band corresponding to each set of surfaces is found to their left, and the color scale bars to their right indicate the relevant patient spectral deviation thresholds (in z-scores). Density plots surrounding each set of surface maps indicate the distribution of spectral amplitude of the cognitively normal group (light blue), averaged bilaterally over the four lobes of the brain. The tick marks below each density plot represent the individual data from the cognitively normal group that was used to generate this distribution, and the vertical dotted lines represent the mean (black) and standard deviations (gray) of these data. The colored points plotted horizontally indicate the comparable patient-level data for each participant in the Alzheimer's disease spectrum group, with cooler colors indicating a greater decrease in amplitude, relative to the cognitively normal group, at that frequency, and warmer colors indicating the inverse.

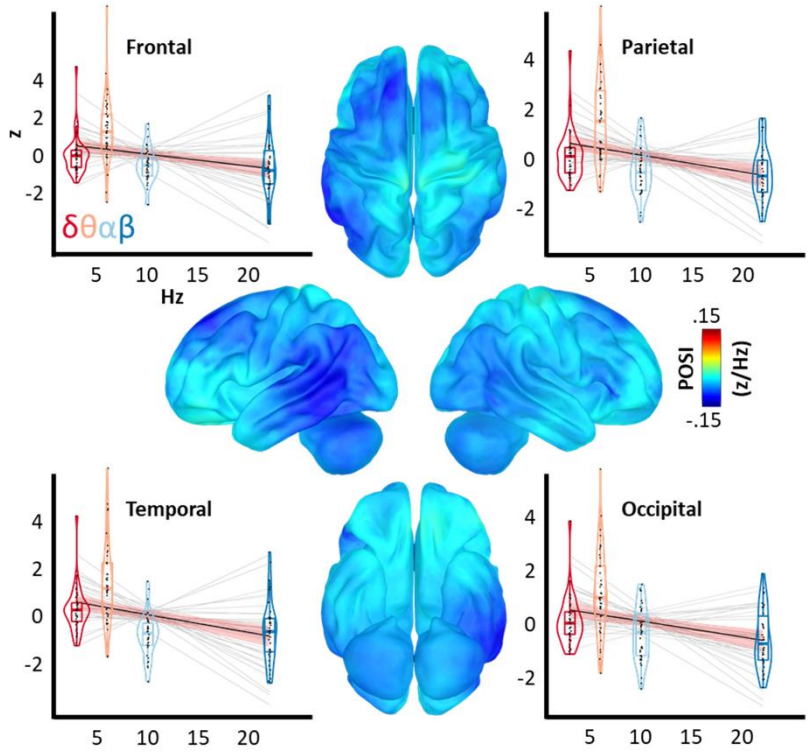

Figure S3. Average spatial patterns of pathological oscillatory slowing in patients on the Alzheimer's disease spectrum. After computation of spatially resolved pathological oscillatory slowing index (POSI) maps for each participant on the Alzheimer's disease spectrum, these maps were averaged across patients to show the subjective spatial pattern of such slowing. The color scale bar on the right indicates the POSI thresholds used for this display (in patient spectral deviations [z]/Hz). Plots surrounding the surface maps represent these POSI scores at the level of each patient, averaged within each lobe of the brain, with frequency (in Hz) on the x-axis and patient spectral deviation (in z) on the y-axis. Light grey lines represent lines of best-fit from the linear model for each patient, and the black line indicates the line of best-fit across all patients, along with the corresponding confidence intervals in salmon. For each frequency band of interest, box plots represent conditional means, first and third quartiles, and minima and maxima, and violin plots show the probability density.

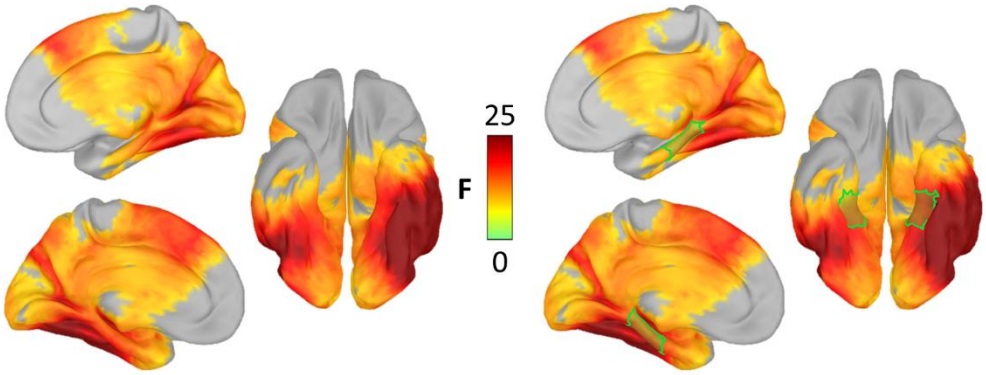

Figure S4. Regions of significant pathological oscillatory slowing in patients on the Alzheimer's disease spectrum, ventral and medial views. Surface maps on the left display the same data as in Figure 2, but with the cerebellum removed and from ventral and medial viewpoints to facilitate interpretation of effects in medial temporal regions. Surface maps on the right display the same effects, but with the parahippocampal cortices highlighted in green.

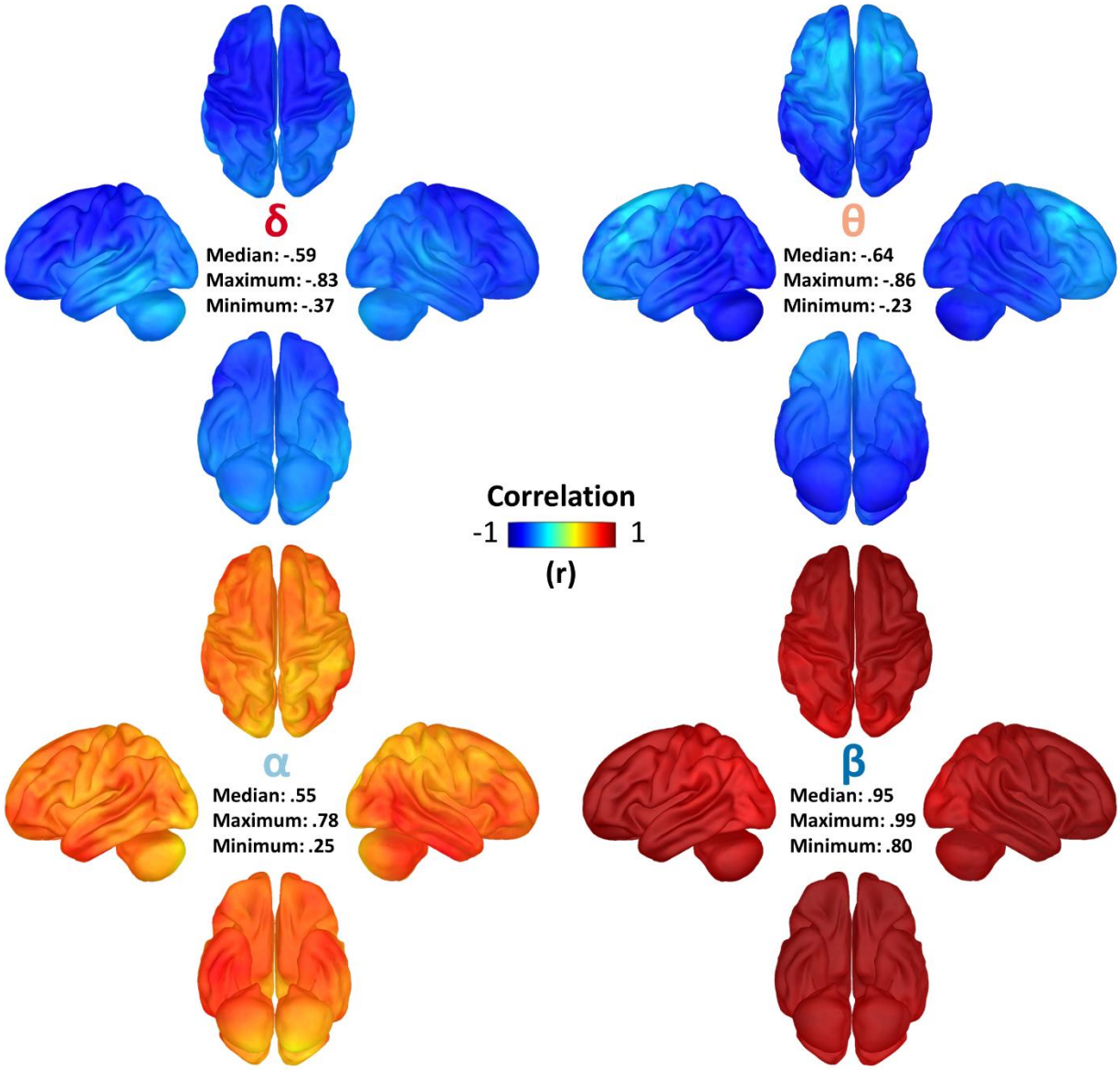

Figure S5. Relative contribution of each frequency band to the inter-participant variability of the pathological oscillatory slowing index. Surface maps indicate the vertex-wise correlation (colorbar; in *r*) of spectral amplitude in each frequency band (indicated by Greek letters in the middle of each set) with the POSI metric, and are meant to display the relative contribution of each band to the inter-participant variability of the POSI metric. The median, absolute maximum, and absolute minimum correlation values are also reported in the middle of each set to aid interpretation.

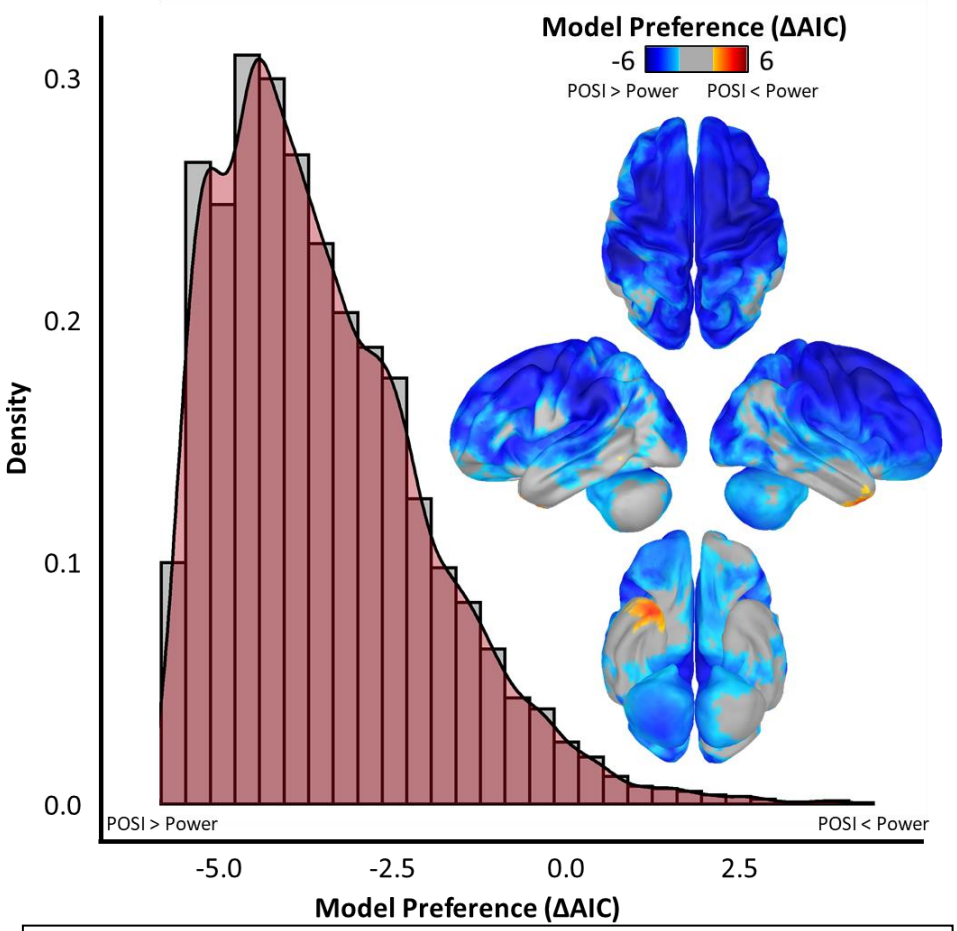

Figure S6. Model comparison of the pathological oscillatory slowing index versus spectral power for predicting general cognitive function. Surface maps to the right indicate results of a vertex-wise model comparison of the POSI metric versus simple derivatives of spectral amplitude (i.e., in the four relevant canonical frequency bands) for predicting general cognitive function (i.e., MoCA scores). The colorbar above represents the results of this comparison in values of ΔAIC (Akaike information criterion), where negative values indicate a better model when using the POSI metric, and positive values indicate the opposite, thresholded at a conservative [ΔAIC] > 3. The histogram to the left indicates the results from the same analysis, but unthresholded and plotted over all modeled vertices, with model preference (in ΔAIC) on the x-axis and the density function plotted on the y-axis.

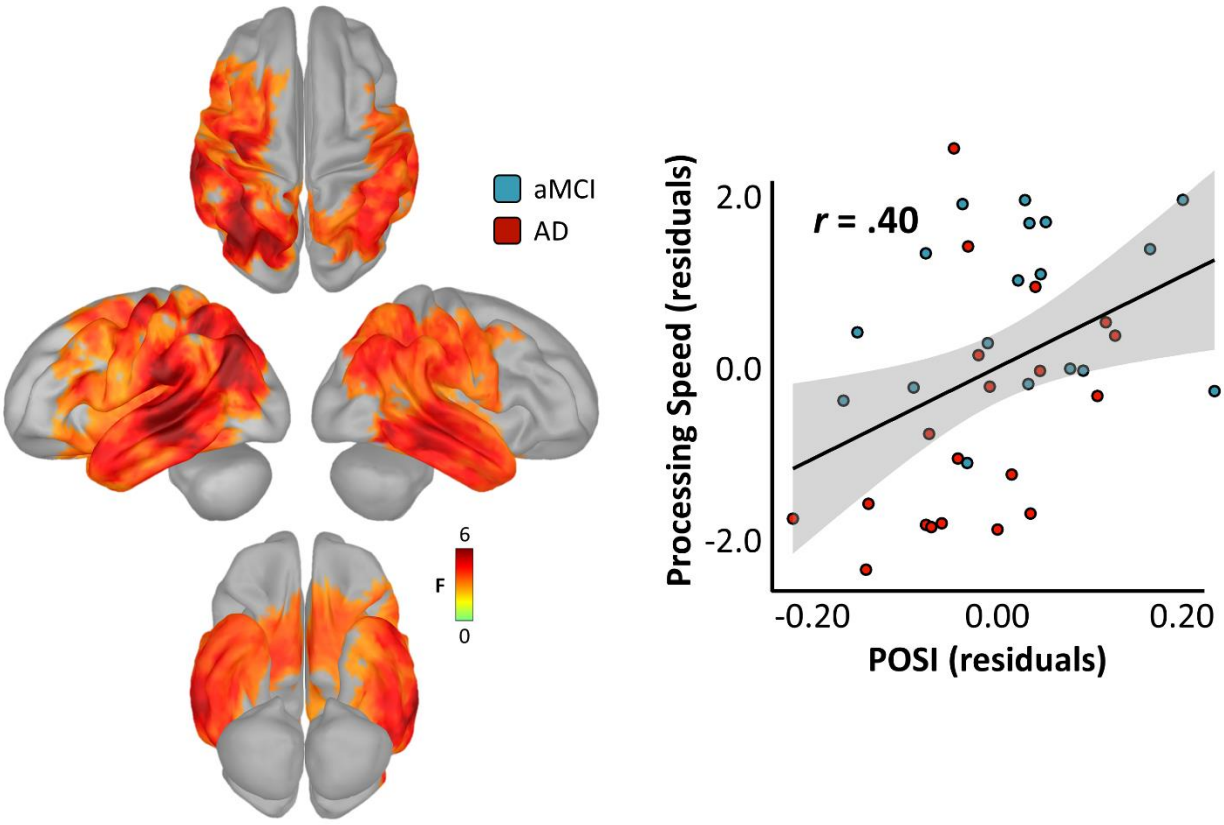

Figure S7. Vertex-wise relationships between pathological oscillatory neuronal slowing and processing speed in patients on the Alzheimer's disease spectrum. Surface maps indicate the results of a regression of the vertex-wise POSI data against processing speed abilities. The color scale bar indicates the statistical (F) values of this test. Importantly, only vertices exhibiting a significant relationship between POSI and processing speed scores (pFWE < .05) are shown in color. The scatterplot to the right of the surface maps represents the POSI-processing speed relationship from the vertex exhibiting the strongest such effect (left IPC; -41, -65, 33), with POSI residuals (in z/Hz) on the x-axis and processing speed residuals (in demographically-normalized z-scores) on the y-axis. The line of best fit for this relationship is overlaid in black, along with the corresponding confidence intervals in gray. The color of each data point indicates clinical determination (blue: aMCI; red: probable AD).

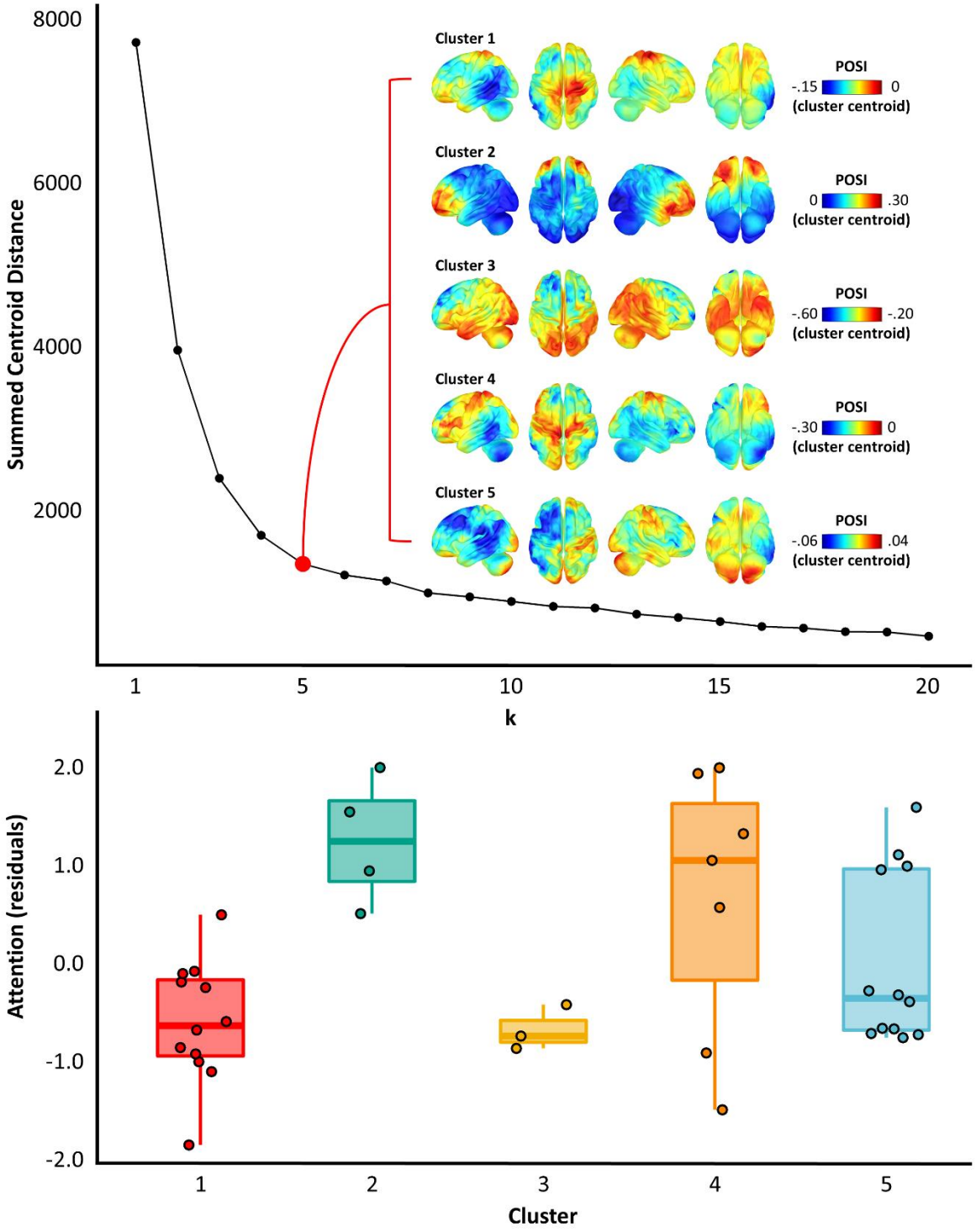

Figure S8. Spatial subtypes of neural slowing in patients on the Alzheimer's disease spectrum. The line plot above (top panel) indicates the results of an analysis to determine the optimal number of clusters (k) for a k-means analysis, with increasing values of k (in # of clusters) plotted on the x-axis and the within-cluster summed centroid distance (in squared Euclidean distance) on the y-axis. A clear "elbow" was apparent at k = 5, and the surface maps of the centroid locations for each of these five clusters are inlaid to the right. Note that the thresholds for these maps were selected so as to facilitate interpretation of the spatial variability within each cluster, but the absolute values of centroid locations (representing the relative slowing at that location for patients with this spatial "subtype") are meaningfully different across clusters (i.e., clusters 1, 3 & 4 are mostly negative, cluster 2 is mostly positive, and cluster 5 is highly variable). The box-and-whisker plot below indicates the results of a significant (p = .004) difference in attentional abilities across these five neural slowing subtypes.

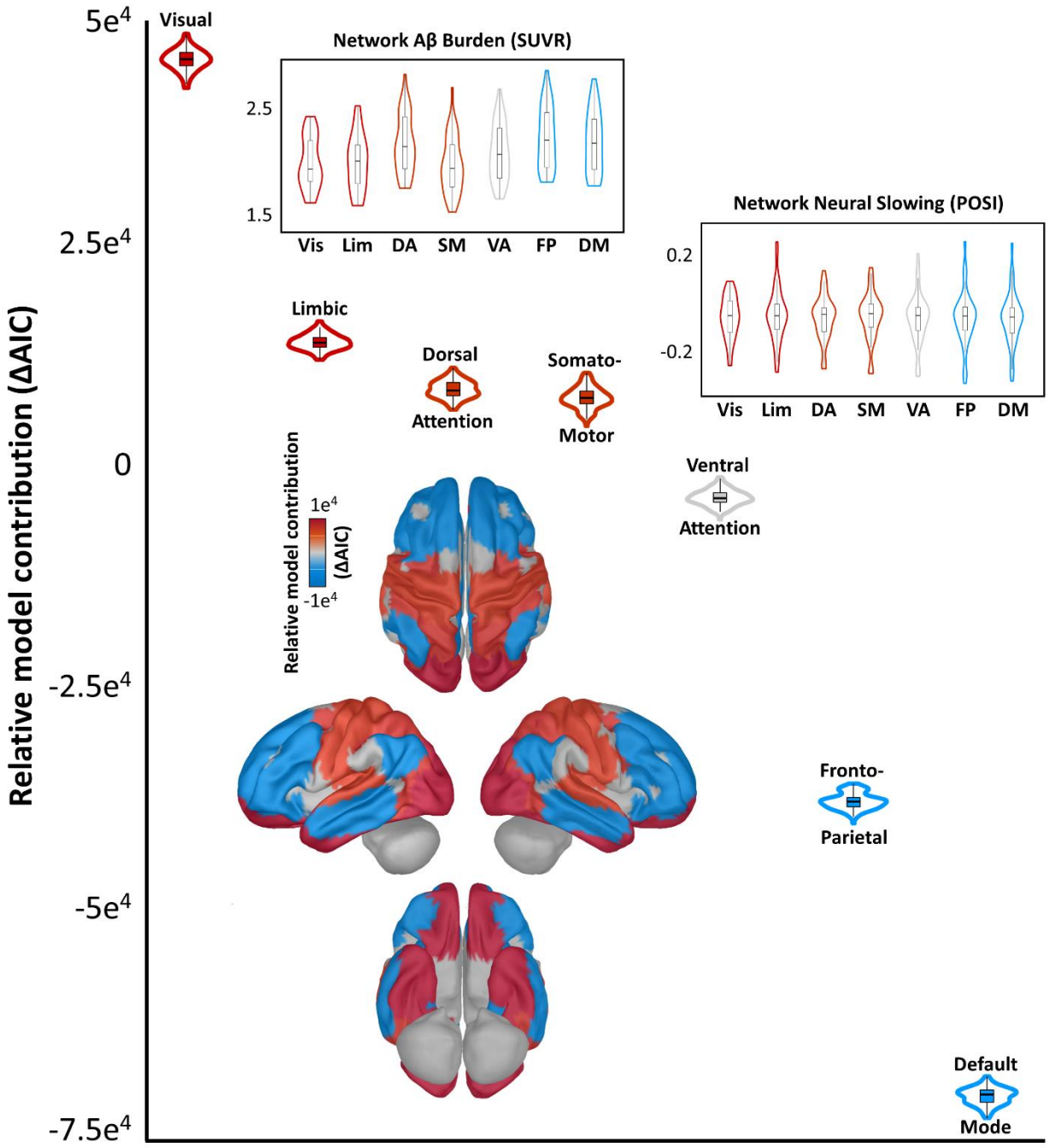

Figure S9. Relative functional network contributions to the neural slowing-Aβ relationship. The larger plot indicates the relative model contribution of each functional network (y-axis, in ΔAIC), relative to 100 equivalently-sized random subsamples of non-network cortex, to the neural slowing-Aβ relationship. Each paired violin/box plot indicates the distribution of ΔAIC values for each network, over the 100 comparisons to random permutations of non-network vertices, with text indicating relevant network labels. Inlaid brain surface maps indicate the mean ΔAIC per each functional network, with warmer colors indicating a larger relative contribution to the neural slowing-Aβ model, and cooler colors indicating the opposite. Inlaid plots above indicate the mean amyloid burden (top left; in SUVR) and mean neural slowing effect (top right; in POSI units [z/Hz]) for each of these networks. For all instances, box plots represent conditional means, first and third quartiles, and minima and maxima, and violin plots show the probability density.

Table S1. Participant demographics and cognitive profiles.

	Age (years)	**Sex** (% female)	**Handedness** (# left)	**Education** (years)	**MoCA**[†]	**MMSE**
CN	72.70 (4.73)	60	1	16.60 (2.87)	27.43 (1.99)	29.20 (1.06)
ADS	69.21 (6.91)*	47	3	15.50 (2.72)	19.13 (4.76)**	23.66 (4.15)**

	Processing Speed	**Attention**	**Memory**	**Learning**	**Verbal Function**
CN	0.66 (0.83)	0.53 (0.60)	0.33 (0.56)	0.60 (0.76)	0.18 (0.76)
ADS	-0.90 (1.42)**	-0.77 (1.06)**	-2.28 (0.70)**	-2.04 (0.88)**	-1.04 (1.01)**

CN: cognitively normal controls; AD: Alzheimer's disease spectrum; MoCA: Montreal Cognitive Assessment; MMSE: Mini-Mental State Exam. Parentheticals for continuous variables indicate one standard deviation. [†]n = 52. *$p < .05$ (ADS vs CN), **$p < .001$ (ADS vs CN).

Table S2. Model comparisons of the Pathological Oscillatory Slowing Index (POSI) versus spectral power for predicting regional amyloid-β burden.

Metric	Relationship to Aβ (t-value)	AIC	ΔAIC (POSI-Metric)
POSI	-61.96**	48395.97	–
Delta Power	-21.89**	51743.51	-3347.54
Theta Power	-3.14*	52211.75	-3815.78
Alpha Power	-31.77**	51214.47	-2818.50
Beta Power	37.14**	50843.90	-2447.93

Aβ: amyloid-β; AIC: Akaike information criterion; POSI: pathological oscillatory slowing index. All models include age as a nuisance covariate. Note that lower AIC values indicate a better model. *$p < .01$, **$p < .001$.

Supplementary Materials and Methods

Positron-Emission Tomography (PET) Processing

PET images were attenuation-corrected using the CT data, reconstructed in MIMNeuro (slice thickness = 2 mm)[1], converted to voxel-wise standardized uptake values based on body weight (SUVbw), and then normalized into MNI space. At this stage, each scan was read by a fellowship-trained neuroradiologist, who was blinded to their group assignment, and assessed as being "amyloid-positive" or "amyloid-negative" using established clinical criteria[1]. Patients who were amyloid-negative were excluded from the AD spectrum group at this point. Images were then normalized to the crus of the cerebellum (SUIT template)[2] to generate voxel-wise maps of SUV ratios[3], and back-transformed into native space using each individual's FreeSurfer-processed T1 MRI data. The PET data overlapping with each individual's cortical gray-matter ribbon was then projected onto a tessellated FSAverage template surface using mri_vol2surf (maximum value; projection fraction = 1; steps of 2)[4], and spatially smoothed (FWHM: 8mm)[5,6].

Neuropsychological Testing

We focused on five cognitive domains impacted in patients with AD: verbal memory (Wechsler Memory Scale-Fourth edition [WMS-IV] Logical Memory II Delayed Recall and Recognition; Hopkins Verbal Learning Test-Revised [HVLT-R] Delayed Recall and Recognition Discriminability Index), learning (WMS-IV Logical Memory I Recall; HVLT-R Learning Trials 1-3), attention and executive function (Wechsler Adult Intelligence Scale-Fourth edition [WAIS-IV] Digit Span Forward, Backward, and Sequencing; Trail Making Test Part B), verbal function (Boston Naming Test; Semantic Verbal Fluency/Animals; Phonemic Verbal Fluency/Controlled Oral Word Association Test), and processing speed (WAIS-IV Coding; Trail Making Test Part A). Demographically corrected test z-scores within each functional domain were averaged to create composite domain z-scores by participant. To corroborate the independence of these domain composite scores, we computed a ratio of z-scores in the cognitively normal group representing the mean of all relationships amongst intra-domain tests, divided by the mean of all relationships with inter-domain tests. All domains had a ratio of $z_{intra}/z_{inter} > 1.50$, and the mean z_{intra}/z_{inter} ratio over all domains was 3.46 (SD = 1.85). This indicates that these domains were ~250% more internally- than externally related. Instrumental activities of daily living (IADLs) were also measured (in collaboration with a spouse or child informant for patients on the AD spectrum) using

the Functional Activities Questionnaire (FAQ)[7], pre-morbid function was assessed using the Wide Range Achievement Test 4 (WRAT-4), and general cognitive status was measured using the Montreal Cognitive Assessment (MoCA)[8] and the Mini-mental State Examination (MMSE) [9].

Head Surface Digitization & Continuous Head Localization

Preceding MEG measurement, four coils were attached to the participant's head and localized, together with the three fiducial points and scalp surface, using a 3-D digitizer (Fastrak 3SF0002, Polhemus Navigator Sciences, Colchester, VT, USA). Once the participant was positioned for MEG recording, an electric current with a unique frequency label (i.e., 293, 307, 314, and 321 Hz) was fed to each of the coils. This induced a measurable magnetic field and allowed each coil to be localized in reference to the sensors throughout the recording session. Since coil locations were also known in head coordinates, all MEG measurements could be transformed into a common coordinate system.

Magnetoencephalography (MEG) Preprocessing

After import into *Brainstorm*, MEG data were bandpass filtered between 1 and 200 Hz and notch filtered at 60, 120, and 180 Hz, and ocular and cardiac artifacts were identified using an automated identification algorithm, supplemented by visual inspection of their temporal and spatial topography. From these artifacts, Signal-Space Projectors (SSPs) were generated for each type of artifact, the temporal and spatial topography of these SSPs were reviewed, and those accounting for expected ocular and cardiac components were removed from the gradiometer data. Artifact-reduced MEG data were then arbitrarily epoched into non-overlapping blocks of 4 s and downsampled to 500 Hz. Epochs still containing major artifacts (e.g., SQUID jumps) were excluded within each participant using the ∪ of standardized thresholds of ± 2.5 median absolute deviations from the median for signal amplitude and gradient.

Spatial Clustering Analysis

To explore the potential clinical relevance of differing spatial patterns of neural slowing, we performed k-means clustering of the spatial POSI data using Matlab's *kmeans* function. The number of clusters was determined by sequentially increasing k from 1 to 20, selecting the solution with the lowest sum of point-to-centroid distances over 10 repetitions for each value of k, and

plotting the resulting point-to-centroid distance sums to identify the value k where these sums reached a point of inflection (i.e., "elbow").[78] Using the optimal k-value identified with this method, we then extracted spatial maps of the centroid approximations per each cluster for visualization purposes. This approach indicated 5 relatively distinct spatial patterns of neural slowing in our patient group (Figure S6, top). To examine the relevance of these spatial patterns for clinical outcomes, we used linear models to test for differences in domain-specific cognitive scores (i.e., memory, learning, attention, processing speed, and verbal function) across these five groups of patients, beyond the effects of age.

References

1. Joshi AD, Pontecorvo MJ, Clark CM, *et al*. Performance characteristics of amyloid PET with florbetapir F 18 in patients with Alzheimer's disease and cognitively normal subjects. *Journal of Nuclear Medicine*. 2012;53(3):378-384.
2. Diedrichsen J. A spatially unbiased atlas template of the human cerebellum. *Neuroimage*. 2006;33(1):127-138.
3. Jack Jr CR, Wiste HJ, Weigand SD, *et al*. Defining imaging biomarker cut points for brain aging and Alzheimer's disease. *Alzheimer's & Dementia*. 2017;13(3):205-216.
4. Fischl B. FreeSurfer. *Neuroimage*. 2012;62(2):774-781.
5. Guo T, Landau SM, Jagust WJ, Initiative AsDN. Detecting earlier stages of amyloid deposition using PET in cognitively normal elderly adults. *Neurology*. 2020;94(14):e1512-e1524.
6. Landau SM, Mintun MA, Joshi AD, *et al*. Amyloid deposition, hypometabolism, and longitudinal cognitive decline. *Annals of neurology*. 2012;72(4):578-586.
7. Pfeffer RI, Kurosaki TT, Harrah Jr C, Chance JM, Filos S. Measurement of functional activities in older adults in the community. *Journal of gerontology*. 1982;37(3):323-329.
8. Nasreddine ZS, Phillips NA, Bédirian V, *et al*. The Montreal Cognitive Assessment, MoCA: a brief screening tool for mild cognitive impairment. *J Am Geriatr Soc*. Apr 2005;53(4):695-9. doi:10.1111/j.1532-5415.2005.53221.x
9. Folstein MF, Folstein SE, McHugh PR. "Mini-mental state": a practical method for grading the cognitive state of patients for the clinician. *Journal of psychiatric research*. 1975;12(3):189-198.